5-2008

Measurement of Absolute Argon Excited State Populations and Electron Energy Distribution Functions in an Ar-a-Si Plasma

Katherine Herring
University of Arkansas, Fayetteville

Measurement of Absolute Argon Excited State Populations and Electron Energy Distribution Functions in an Ar-a-Si Plasma

Honors Thesis

Katherine Herring

28 April 2008

Abstract

Deposition systems utilizing plasma are used for a variety of tasks, including tool coatings and creating thin-film materials. In order to have repeatable results, the internal conditions of a plasma chamber need to be known. This project centered on the use of data from optical emissions and a Langmuir probe from an argon plasma amorphous silicon depositing system. An electron energy distribution function (EEDF) was obtained from manipulation of the Langmuir probe data. This EEDF was then input to an argon collisional-radiative model (CRM) to obtain the electron population of the 4p level of the argon plasma. Through an absolute calibration, the same 4p population will be studied by the optical emissions experiment. The result from the Langmuir study was that the 4p population was $5x10^{13}$ m^{-3}, while the optical emissions result was $2x10^{13}$ m^{-3}. These are reasonably close values, well within a range of verification, but further study needs to be done to confirm these results.

Plasma chamber deposition systems are used in coating various tools and devices, such as alpha-alumina on tool bits and orthopedic devices, in the creation of thin-layer materials, as in the case of amorphous silicon (a-Si), and many other applications. Amorphous silicon has many applications, but is mostly used for liquid crystal displays and large-area solar energy cells. The system used in this study is an a-Si deposition chamber, specifically an R&D plasma system designed by MVSystems, Inc. While the deposition was not utilized or studied during these experiments, the development of techniques for characterization of the plasma is valuable in producing repeatable results of a desired a-Si quality.

Generally, Plasma is made by using a power source to excite molecules of a gas, in our case argon. This argon plasma is full of excited electrons, ions, and neutral particles. These particles quickly reach a steady state, where the number of electrons being excited equals the number that fall back to lower levels to keep the neutral charge of the plasma. To the right is a chart that has the different energy levels electrons can belong to in an argon atom [1]. These different levels are well known and the probabilities for electrons belonging to these different levels are relatively easy to

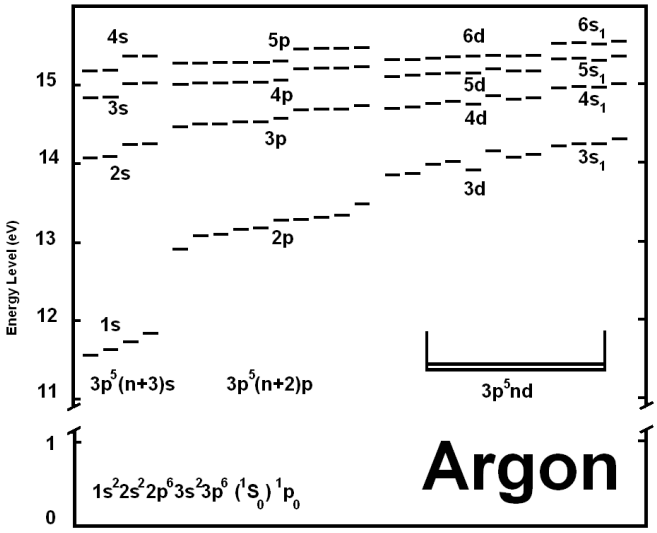

Figure 1 - Argon Electron Energy Levels

calculate. Describing a model for the energy of these electrons can be used following a Maxwellian electron energy distribution function (EEDF) if the plasma is at thermal equilibrium. Thermal equilibrium is difficult to achieve. Since the electrons in the plasma have such smaller mass than ions, they heat much faster and interact with other species more rapidly. These temperature differences are what cause the system to be categorized as non-Maxwellian. Our system is not at equilibrium and therefore we follow a non-Maxwellian approach to our EEDF, which describes the plasma through the average energy of the ions and electrons, rather than simplifying these energies down to their equilibrium levels, as could be done if the system were Maxwellian. This is what is meant by a collisional-radiative model (CRM). The probabilities of electrons populating certain levels are calculated based on inputs of conditions in the chamber, which then gives enough information to determine the excited state population density of the different energy levels.

The CRM used in this study was produced by a former PhD student in the University of Arkansas Mechanical Engineering department [2]. The different levels of electrons are merged together into average conglomerations of the levels in his model. What this means is that for each electron level, there may be several sublevels and many electrons contained therein. The way the CRM handles these multiple species is to average the energies. For example, the 4p electron level has 6 different sub-levels, but these are all averaged into one 4p population.

A Langmuir probe was used to find the population density of electrons and ions inside the plasma at the center of the reaction chamber. The probe can be moved to find these densities at any point along an axis in the chamber. Measuring at the center of the

reaction chamber gives a good average for what is happening, and is what was done in this experiment. By applying different potentials to the probe, it attracts either ions or electrons to it. A negative potential will attract the positively charged ions and a positive potential will attract the negatively charged electrons. These attractions are recorded by the probe as a current, which can then be used to find the electron energy distribution functions (EEDFs) through mathematical manipulation of the data. This EEDF is then used as input to the CRM mentioned above to find the 4p population.

Alongside the Langmuir probe experiment, optical data was taken from the chamber through the use of a fiber optic sensing system. The fiber optic system catches the light coming off the plasma. This light represents the energy of the electrons falling to lower energy levels from higher energy levels. The sensing system records values of intensity of the light at different wavelengths, which can tell us what energy level these electrons belong to. The National Institute of Standards and Technology (NIST) database gives known values from countless experiments of what atoms these electrons should belong to and the energy of the electrons based on the wavelength at which the intensity peak was found. The NIST database also gives other information concerning the specific intensity line which was needed in the calculations made, including the Einstein transition probability and the degeneracy. The end result of the optical emissions calculation is a measurement of the 4p population.

A 4p population can give the needed information to calculate the ground state electron population, which cannot be measured directly and is useful in determining what reactions will happen inside the plasma chamber. Having the ground state electron population will characterize the specific conditions in the chamber in a unique form. In

this way, if a particular result with the a-Si deposit needs to be reproduced, analyzing the ground state population would be a good way to determine that the conditions in the chamber are exactly right.

Experiment

Optical emissions spectroscopy (OES) and the utilization of a Langmuir probe are common methods for characterizing plasmas [3-6]. OES is an extremely easy, relatively fast and very unintrusive method of data collection for analyzation of plasma chambers. Relative calibration is often used in most OES studies [7]. This study as well as others uses an absolute calibration to compare against a CRM [11]. Absolute calibration differs from relative calibration in that the experimental setup for the calibrations step and the plasma chamber data collection are exactly the same. By utilizing the same setup, the exact energy levels are known, rather than just having the knowledge that one level's energy in relation to other levels. The Langmuir probe is used to find the electron density of the plasma as well as for deriving an EEDF. There are commercially available programs that can estimate these values, such as ELENDIF, but direct measurement by probe is preferable [8,9].

Our system was an a-Si deposition chamber in a multi-chamber R&D system designed by MVSystems, Inc. This was a radio frequency magnetron plasma run at 150W and 5 mTorr, with an argon flow rate of 20 sccm.

As mentioned before, since an absolute calibration was used, the exact setup for taking OES data was utilized for measurement of the calibration and the plasma chamber

itself. Data were taken from 350 to 1000 nm using an OceanOptics USB 4000 CCD. A viewport on the side of the plasma chamber was used to capture light, and a 50 W tungsten lamp source was used for the calibration. In order to keep an identical setup, an optical breadboard was used to assemble the array of lenses needed to focus the light into the fiber optic cable used for input into the computer system. Figure 2 shows a diagram of the setup used.

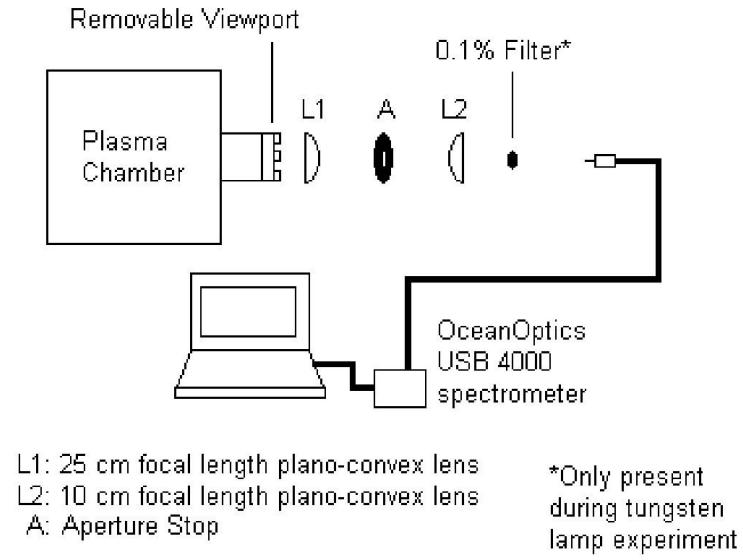

Figure 2 - Setup for OES Data Collection

A 25 cm focal length plano-convex lens with planar side facing the chamber, an aperture stop, and a 10 cm focal length plano-convex lens with planar side aimed away from the chamber were assembled on the breadboard. They were calibrated so that the lenses were centered on the viewport and the end of the fiber optic cable was centered on the other side of the setup. During the tungsten lamp calibration, the lamp was placed approximately the same distance away from the 25 cm focal length lens as the center of the plasma, and a 0.1% filter was inserted into the setup. The filter was needed because

of the relatively bright intensity of the lamp in comparison to the plasma chamber glow. If it was not used, the CCD array would have been constantly saturated, giving unusable results. The data was taken from the tungsten lamp at an integration time of 75,000 μs, while the plasma chamber data was taken at an integration time of 100,000 μs. Neither of these differences would affect the integrity of the absolute calibration, as they can be corrected during the calculation phase of the experiment.

The last piece of data needed to complete the absolute calibration is the temperature of the system. To calculate this, we use a Pyro-micro vanishing filament optical pyrometer to get readings of temperature versus emissivity for the tungsten bulb which can then be used to find the temperature of the system.

Separately, the Langmuir probe was used to gather data on the electron density of the plasma. A tungsten tip, 10 mm in length and 0.15 mm in diameter was used for the Langmuir probe data collection. Before calculations were performed, the data were smoothed using digital filters. This is important, as noisy data will produce poor results as calculations will expand small deviations to very large deviations. The electron density was estimated from the slope of the electron saturation current [14].

Because the system has only one viewport, the OES and Langmuir probe data could not be taken concurrently. However, since the system produces repeatable results within a 5% margin of error, this method for acquiring the data at different times was found to be acceptable.

Theory

The absolute calibration depends on a few important equations. The first is that of the excited-state density, n_m. This value is found through Equation 1, which relates the density to the true plasma intensity, I_{mn}, the known wavelength of transition λ_{mn}, and the Einstein transition probability, A_{mn}:

$$n_m = \frac{4\pi I_{mn}\lambda_{mn}}{hcA_{mn}}$$

Equation 1 - Excited State Density

where h is Planck's constant and c is the speed of light.

A_{mn} is obtained in this study from the NIST database [13], but the other unknown, I_{mn}, is found through the use of the absolute calibration. The relationship of I_{mn} to data taken from the system is given in Equation 2.

$$I_{mn} = \frac{V_{plasma}}{D_\lambda}$$

Equation 2 – True Plasma Intensity

where V_{plasma} is the reading of counts for a particular wavelength of the plasma and D_λ is the conversion factor to convert this count reading from a known source (lamp) to the desired source (plasma). Equation 2 is most of what the absolute calibration boils down to.

The conversion term D_λ is described by Equation 3:

$$D_\lambda = \frac{V_{lamp} d_{plasma}}{\varepsilon(\lambda,T)\left(\frac{2hc^2}{\lambda^5\left(e^{\frac{hc}{\lambda kT}}-1\right)}\right)\left(\frac{d\lambda}{dx}\right)w_{exit}}$$

Equation 3 - Intensity Conversion Factor

where d_{plasma} is the depth of the plasma, $d\lambda/dx$ is the linear dispersion of the spectrophotometer, and w_{exit} is the width of the exit slit of the spectrometer. On the bottom of the equation for D_λ is Planck's function for intensity. There are constants h, Planck's constant, k, Boltzmann's constant, and c, the speed of light. By calculating this term, the response of the spectrometer is now known. This means that since the spectrometer was used on a known emitter, the response of the spectrometer for other, unknown sources can now be calculated.

T in Equation 3 is the temperature of the tungsten source, found using an optical pyrometer in conjunction with emissivity values from Larrabee (Equations 4, 5, and 6) [12].

$$\varepsilon(\lambda,T) = 0.6075 - 0.3\lambda - 0.3265x10^{-4}T + 0.59x10^{-4}\lambda T \quad (0.350\ \mu\text{m} - 0.450\ \mu\text{m})$$
$$\varepsilon(\lambda,T) = 0.4655 + 0.01558\lambda + 0.2675x10^{-4}T - 0.7305x10^{-4}\lambda T \quad (0.450\ \mu\text{m} - 0.680\ \mu\text{m})$$
$$\varepsilon(\lambda,T) = 0.6552 - 0.2633\lambda - 0.7333x10^{-4}T + 0.7417x10^{-4}\lambda T \quad (0.680\ \mu\text{m} - 0.800\ \mu\text{m})$$

Equations 4-6 - Larrabee Equations

The pyrometer was used to find emissivity versus temperature for the tungsten light source. The values found from this data collection are on the next page in Table 1.

Emissivity	Tu (K)	Tε (K)
0.38	2721	3091
0.39	2719	3078
0.40	2721	3069
0.41	2719	3056
0.42	2719	3046
0.43	2721	3038
0.44	2720	3028

Table 1 - Pyrometer Data

The linear regression of this data is found and then plotted against that of the applicable Larrabee equation. The effective wavelength of the pyrometer used is 655 nm. This value is used in Equation 5 to plot a linear function. The intersection of Equation 5 and the linear regression of the data in Table 1 is the temperature of the system and is shown below in Figure 3.

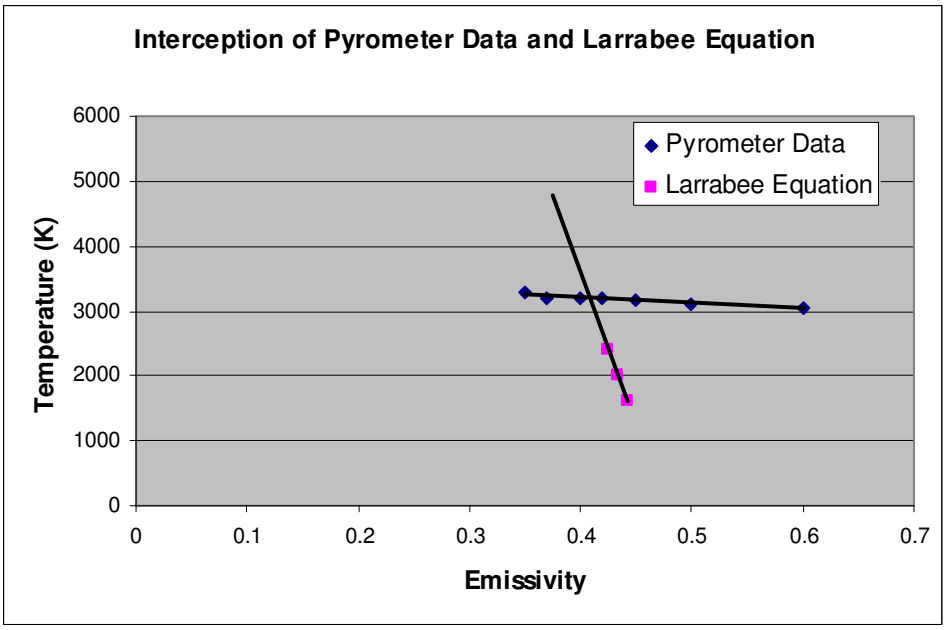

Figure 3 - Interception of Pyrometer Data and Larrabee Equation

After the required variables are found and the density of the excited state is known, these values can be compared to those found through the use of the CRM with data from the Langmuir probe. All needed transition data are found through the NIST database and are provided in Table 2.

Wavelength (nm)	A_{ki} (s^{-1})	g_k	ε_k (eV)
751.4651	4.02E+07	1	13.2730373
763.5105	2.45E+07	5	13.1717769
801.4785	9.28E+06	5	13.0948717
811.5311	3.31E+07	7	13.0757149
842.4647	2.15E+07	5	13.0948717
912.2967	1.89E+07	3	12.9070145

Table 2 - NIST Database Values

Results and Discussion

Figure 4 on the next page shows the uncorrected data collected from the plasma chamber. A second collection of data with the chamber turned off was taken in order to get the background light from the room. This background signal is then subtracted from the raw data.

The emission data from the tungsten lamp required three corrections. The first was to correct for the assumption in our calculations that the lamp is a solid emitter. The tungsten lamp has a series of coils that emit light, and so what is needed for this correction is a determination of what the lamp would emit were it a solid emitter. For this, it was estimated that the surface coil to solid ratio of the lamp is 0.625. The data taken from the system are therefore multiplied by the reciprocal of this relationship to

increase the signal to that which would be expected had the lamp actually been a solid emitter. The second was a correction for the difference in integration time between the lamp data acquisition and the chamber data acquisition. This correction is also simple, as the intensity is multiplied by the ratio of the integration time for the plasma chamber to the integration time of the tungsten lamp. The third was a correction for the filter that was in place for the lamp setup but not the chamber setup. This filter was needed because the lamp signal was too strong for the CCD detector when optimized to record the relatively weak plasma signal. This also just required a multiplier to correct.

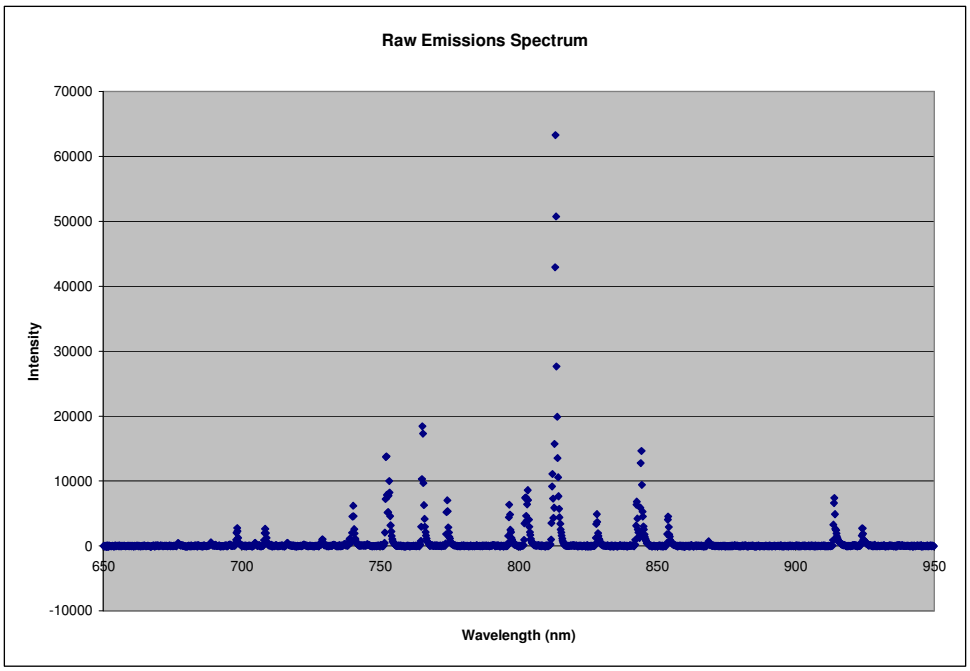

Figure 4 - Raw Emissions Spectrum

As outlined in the theory section, the densities of the atomic excited states were calculated. Figure 5 on the next page shows these data and indicates that the absolute densities are in the 10^{13} and 10^{14} m^{-3} range. Since the CRM groups all 4p states into one

super-state at 13.171eV, we use the 763.5nm transition for comparison ($2x10^{13}$ m^{-3}). Note that for reference, a best fit line is also included.

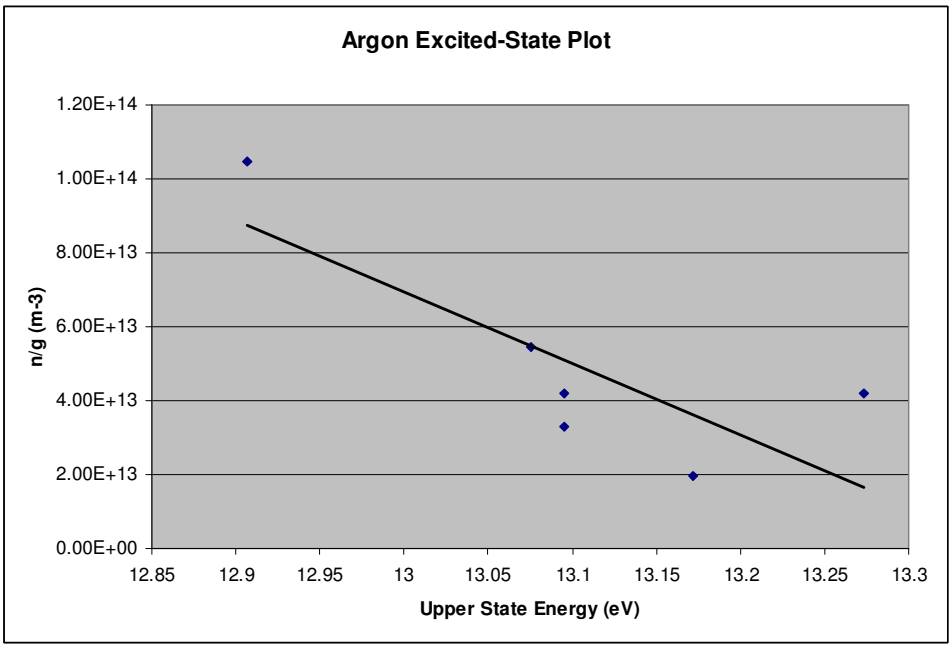

Figure 5 - Argon Excited-State Plot

The Langmuir probe was used to obtain an electron energy distribution function to input to the CRM. The CRM only accounts for argon in the plasma, but although there will be some silicon sputtered into our plasma, there have been previous studies conducted under similar conditions with this CRM with good results [10]. The EEDF from the Langmuir probe that was used as input for the CRM is shown in Figure 6. The measured electron density from the probe was $1.8x10^{16}$ m^{-3}.

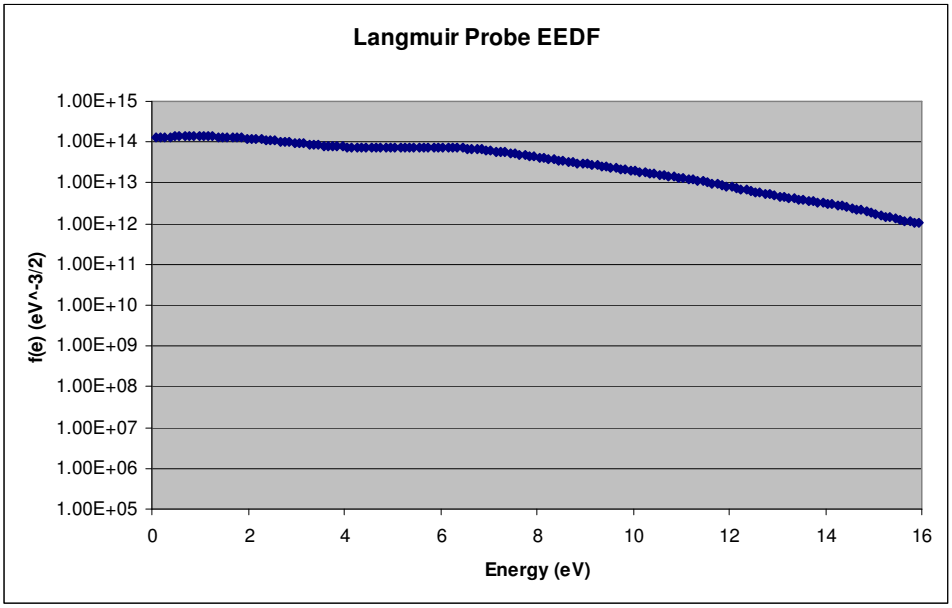

Figure 6 - Langmuir EEDF

The CRM output contains 25 electron energy levels, but the 4p population that we are interested in is a conglomeration of all the different 4p states. As mentioned before, the 763.5nm line from the absolute calibration is used to estimate the 4p population. This estimation stems from the average energy of the 4p state from the CRM being 13.171eV, the same as the upper state energy of the 763.5nm line. From the OES, the 4p population was estimated to have an absolute density of $2x10^{13}$ m^{-3}, while the population was estimated at $5x10^{13}$ m^{-3} from the CRM. These values are also in the range that is expected, as found from previous research [9, 10].

Conclusions

From the analyzation of OES and Langmuir probe data, a comparison can be made of the 4p excited-state population of the Ar a-Si plasma chamber. The 4p

population was found to be $2x10^{13}$ m^{-3} from the absolute calibration of the OES data, while the 4p population was found to be $5x10^{13}$ m^{-3} from the CRM output that is based on the Langmuir probe data. These two values seem to match well, and it is hoped that further measurements can be performed to help characterize the plasma created in this chamber in order to improve the quality of a-Si formed in this chamber.

References

[1] E.J. Chilton, "Measurement of electron-impact excitation into the 3p54p levels." Phy. Rev. A, 57, 267-277, 1998.

[2] U.M. Kelkar, "Diagnostic and Modeling in Nonequilibrium Microwave Plasmas", PhD Thesis, Uni. Of Arkansas, Fayetteville AR (1997).

[3] Y.M. Kim, Y.M. Chung, M.J. Jung, J. Vlcek, J. Musil, and J.G. Han, "Optical emission spectra and ion energy distribution functions in TiN deposition process by reactive pulsed magnetron sputtering," Surf. Coat. Technol., 200, 835, 2005.

[4] J. Vlcek, K. Rusnak, and V. Hajek, "Reactive magnetron sputtering of CN_x films: Ion bombardment effects and process characterization using optical emission spectroscopy," J. Appl. Phys., 86 (7), 3646, 1999.

[5] D.-C. Seo and T.-H. Chung, **"**Observation of the transition of operating regions in a low-pressure inductively coupled oxygen plasma by Langmuir probe measurement and optical emission spectroscopy," J. Phys. D: Appl. Phys., 34 (18), 2854, 2001.

[6] A. Vetushka, S.K. Karkari, and J.W. Bradley, "Two-dimensional spatial survey of the plasma potential and electric field in a pulsed bipolar magnetron discharge," J. Vac. Sci. Technol., A 22 (6), 2459, 2004.

[7] A.D. Srivastava, M.H. Gordon, and D.G. Bhat, "Optical emission spectroscopy in an inverted cylindrical magnetron plasma," Surf. Coat. Technol., 200, 1346, 2005.

[8] W.L. Morgan and B.M. Penetrante, "ELENDIF: A time-dependent Boltzmann solver for partially ionized plasmas," Comput. Phys. Commun., 58 (1-2), 127-152, 1990.

[9] V.M. Donnelly et al, "Optical plasma emission spectroscopy of etching plasmas used in Si-based semiconductor processing," Plasma Sources Sci. Technol., 11 (3A), A26-A30, 2002.

[10] P. Lipka, S. Mensah, M. H. Gordon, and D. Bhat, "Absolute argon excited-state population measurements from emission spectroscopy in an inverted cylindrical magnetron plasma," Surf. Coat. Technol., 202, 910-914, 2007.

[11] R. Kashiwazaki and H. Akatsuka, "Effect of Electron Energy Distribution Function on Spectroscopic Characteristics of Microwave Discharge Argon Plasma," Jpn. J. Appl. Phys., 41 (8), 5432-5441, 2002.

[12] R.D. Larrabee, "Spectral emissivity of tungsten," J. Opt. Soc. Am. 49 (6), 619, 1959.

[13] http://physics.nist.gov/PhysRefData/ASD/index.html.

[14] J. Rubinstein and J. G. Laframboise, "Upper-bound current to a cylindrical probe in a collisionless magnetoplasma," Phys. Fluids, 21, 1655, 1978.